PCCP

The structure of *N*-aminopyrazole in the solid state and in solution: an experimental and computational study

José Antonio Jiménez,[a] Rosa María Claramunt,*[a] Otilia Mó,[b] Manuel Yáñez,[b] Frank Wehrmann,[c] Gerd Buntkowsky,[c] Hans-Heinrich Limbach,*[c] Richard Goddard*[d] and José Elguero[e]

[a] *Departamento de Química Orgánica y Biología, Facultad de Ciencias, UNED, Senda del Rey 9, E-28040 Madrid, Spain*
[b] *Departamento de Química C-9, Facultad de Ciencias, Universidad Autónoma de Madrid, E-28049 Cantoblanco, Madrid, Spain*
[c] *Institut für Chemie, Freie Universität Berlin, Takustrasse 3, D-14195 Berlin, Germany*
[d] *Max-Planck-Institut für Kohlenforschung, Kaiser-Wilhelm-Platz 1, D-45470 Mülheim an der Ruhr, Germany*
[e] *Instituto de Química Médica, CSIC, Juan de la Cierva, 3, E-28006 Madrid, Spain*

Received 30th July 1999, Accepted 28th September 1999

The title compound *N*-aminopyrazole (AMPZ) has been studied both theoretically and experimentally using *ab initio* methods, low-temperature X-ray crystallography, differential scanning calorimetry, IR spectroscopy, liquid state ^{1}H NMR, broadband solid state ^{2}H NMR and high resolution solid state ^{15}N NMR spectroscopy, focussing on the structure and dynamics of the amino group and the characteristics of hydrogen bond (HB) association. The complete amino group rotation–inversion surface of AMPZ and, for comparison, also of the aniline monomer were calculated at the B3LYP/6-31G* level. The results indicate that monomeric AMPZ exhibits an sp^3 hybridized pyramidal amino group where the HH-distance vector is located perpendicular to the pyrazole ring and the hydrogen atoms bent towards the pyrazole ring nitrogen atom, *i.e.* with the lone electron pair *anti* to the latter. Both inversion at the nitrogen atom and the 180° rotation of the amino group lead to a metastable structure, where the inversion barrier is much larger than the rotational barrier. These results contrast with those obtained for aniline where the amino group is almost planar and subject to a degenerate 180° rotation. Further calculations of the hydrogen bonded cyclic AMPZ dimer indicate that hydrogen bond association does not substantially perturb the geometry of the amino group, where one of the amino group protons and the ring nitrogen atoms are involved in hydrogen bonding. The X-ray structure was determined at −173 °C (100 K) on a monocrystal obtained by zone crystallization. DSC shows that on cooling, neat liquid AMPZ exhibits a solid–solid phase transition around −45 °C to a low-temperature phase. In this phase AMPZ forms a weakly hydrogen bonded chain where the structure is similar to the one calculated for the monomer. Only one of the amino protons is involved in hydrogen bonding, where the NH stretch of the hydrogen bonded proton appears at 3197 cm^{-1} and of the non-hydrogen bonded proton at 3314 cm^{-1}. Solid state ^{2}H NMR spectroscopy of [ND_2]AMPZ shows low-temperature structures with rigid ND vectors below and isotropically rotating vectors above the solid–solid phase transition. Hydrogen bond association was further studied by solid state ^{15}N CPMAS (cross polarization magic angle spinning) NMR and by low-temperature liquid state ^{1}H NMR of AMPZ specifically ^{15}N labelled in the amino group. In contrast to the solid state, hydrogen bond exchange rendering the two amino group protons equivalent was found to be fast in the NMR timescale even at 100 K.

1. Introduction

This paper addresses a feature that is probably unique to heterocyclic chemistry and that is the bond between the N(1) atom of an azole (an aromatic five-membered ring containing at least one nitrogen atom)[1] and its R substituent. In contrast to the C–R bond in aromatic heterocyclic compounds, which in its reactivity only differs by a small amount from that of aromatic compounds, the N(1)–R bond has no counterpart in any other part of organic chemistry. It has been qualitatively compared by Kauffmann to a halogen–R bond because the azoles are good negative leaving groups, and indeed, azoles, when linked by the nitrogen, have been classified as pseudo-halogens.[2] It is also the reason why *N*-acylazoles (azolides) are good acylating groups, *e.g.* acetyl chloride, and why they react very differently from their equivalent acetophenones or acetylpyridines.

We address in this paper the structural and dynamic properties of 1-aminopyrazole **1** (AMPZ) in the solid state and in solution, where aniline **2** will serve partly as a reference (Scheme 1). AMPZ belongs to the family of *N*-aminoazoles which have received much attention both for their interesting reactivity and for their spectroscopic properties.[3] The only structural information available for **1** comes from theoretical studies, both semiempirical (INDO)[4] and *ab initio* (MP2//6-31G**).[5] All calculations agree that the most stable conformation, at least for the isolated molecule, is the *antiperiplanar* one, as represented in Scheme 1. In Scheme 1, we have included the other simple aminoheterocycle, 2-aminopyridine **3** which is a much better studied compound. It is a near-

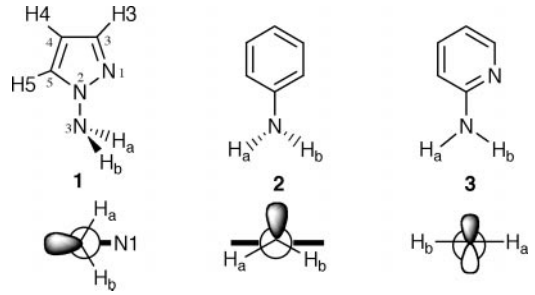

Scheme 1

planar molecule (X-ray structure determination),[6] with a high rotational barrier about the C–N bond (32 kcal mol^{-1} for the *N*,*N*-dimethyl derivative)[7] and has been the subject of many theoretical studies.[8]

All three compounds are primary aromatic amines and represent hydrogen bond donors, but **1** and **3** contain in addition a proton acceptor nitrogen site leading potentially to the formation of cyclic dimers, such as nucleic acid bases, or to linear chains, catemers. The hydrogen bond (HB) association of AMPZ has not yet been addressed in the literature to the best of our knowledge, neither in solution nor in the solid state. Note that in this paper we have not used the standard numeration of AMPZ [with N(1) the atom bearing the amino group] but a correlative numbering of the three nitrogen atoms (Scheme 1).

This paper is organized as follows. After an experimental part describing the synthesis of AMPZ and other experimental details, we present (1) a theoretical study of the AMPZ monomer, (2) a theoretical study of the AMPZ dimer in order to understand its behavior in condensed matter, (3) the results of combined X-ray, DSC, IR and NMR studies for obtaining information about the structure of solid AMPZ, and (4) the results of a liquid state NMR study of AMPZ in solution.

2. Experimental

2.1 Synthesis of the labelled compounds

Synthesis of [^{15}N]hydroxylamino-*O*-sulfonic acid.[9] From 2 g (0.028 mol) of [^{15}N]hydroxylamine hydrochloride, 3.015 g (94%) of [^{15}N]hydroxylamino-*O*-sulfonic acid were obtained. The purity of the compound was checked by iodimetric titration and was found to be >98%.

Synthesis of [$^{15}NH_2$]-1-aminopyrazole ([^{15}N]AMPZ).[10] In a 50 mL round-bottomed flask was placed a solution of 0.613 g (0.009 mol) of unlabelled pyrazole in 16 mL of aqueous sodium hydroxide (2.4 g, 0.06 mol). The solution was heated to 50 °C and 3 g (0.026 mol) of [^{15}N]hydroxylamino-*O*-sulfonic acid were added in small quantities while avoiding the temperature rising above 60 °C (60–90 min). After the addition was completed, the mixture was stirred at room temperature for another 30 min. The resulting solution was extracted with chloroform (3 × 25 mL). The organic layer was washed with water and dried over anhydrous sodium sulfate. The solvent was eliminated under vacuum and the residue was purified by column chromatography over alumina using $CHCl_3$ as eluent (aluminium oxide 90 active, neutral, activity I, 70–230 mesh ASTM, $R_f = 0.32$) followed by distillation (bp 71 °C/15 Torr), yield 0.574 g, 76%. Its melting point will be reported later on (Section 3.3).

Synthesis of [ND_2]-1-aminopyrazole ([ND_2]AMPZ). Using the standard procedure to exchange mobile NH protons,[11] AMPZ (500 mg) was dissolved in CH_3OD (5 mL) and then evaporated to dryness. If necessary the procedure was repeated again. The product should be kept sealed and exposed the shortest time to atmosphere.

2.2 X-ray structure determination

Attempts to grow suitable crystals of 1-aminopyrazole for an X-ray analysis from solution were unsuccessful and a single crystal was eventually grown from the melt. 1-Aminopyrazole[10] was purified by vacuum distillation, and 2 μL of the compound were introduced under argon into a 0.5 mm diameter glass capillary (glass No. 50, Hildgenberg), which was sealed using a narrow H_2 flame. The sample was mounted on an Enraf-Nonius CAD4 diffractometer and cooled by a cold stream of N_2 gas. A single crystal was grown by zone crystallization directly on the diffractometer at −10 °C using a CO_2 laser to melt the sample (mp −0.76 °C). The melted region was drawn repeatedly from the top to the bottom of the capillary at a rate of 0.05 mm h^{-1} until a single crystal was obtained.

Crystal data for 1.† $C_3H_5N_3$, $M_r = 83.10$ g mol^{-1}, colorless rod, crystal size 0.61 × 0.48 × 0.48 mm, $a = 10.468(7)$, $b = 13.484(3)$, $c = 5.755(1)$ Å, $U = 812.3(6)$ Å^3, $T = 100$ K, orthorhombic, *Pccn* [No. 56], $Z = 8$, $d_{calc} = 1.36$ g cm^{-3}, $\mu = 0.10$ mm^{-1}, Enraf-Nonius CAD4 diffractometer, $\lambda = 0.71069$ Å, $\omega - 2\theta$ scan, 3420 reflections, 935 independent, 797 observed [$I > 2\sigma(I)$], $[(\sin\theta)/\lambda]_{max} = 0.65$ $Å^{-1}$, direct methods (SHELXS-97),[12] least-squares refinement (on F_0^2),[13] H isotropic, 76 refined parameters, $R = 0.058$ (obs. data), $R_w = 0.144$ (Chebyshev weights), final shift/error 0.001, residual electron density +0.439/−0.382 e$Å^{-3}$.

2.3 DSC

DSC experiments were carried out on a SEIKO DSC 220C, connected to a Model SSC5200H Disk Station. The temperature scale was calibrated against the melting points of high purity indium and tin. A thermogram of AMPZ (distilled under argon atmosphere), contained in a hermetically sealed aluminium crucible, was recorded over the entire temperature range under argon atmosphere at the scanning rate of 2.0 °C min^{-1}. The sample size was 3–10 mg.

2.4 IR spectroscopy

The IR spectra were recorded on a FT-IR Bomem-DA3 spectrophotometer using a Globar infrared source and a detector of deuterated triglycine sulfate (DTGS). The spectral resolution is 0.89 cm^{-1}.

2.5 NMR experiments

^{2}H and ^{1}H solid state NMR. All ^{2}H and ^{1}H NMR experiments were performed on a home built spectrometer at a field of 6.98 T,[14] corresponding to a ^{2}H resonance frequency of 45.7 MHz on a standard Oxford wide bore magnet (89 mm) equipped with a room temperature shim unit. For the ^{2}H-channel a 2 kW class AB amplifier from AMT and for the ^{1}H-channel a 1 kW class C amplifier from Creative Electronics were employed. Both amplifiers are equipped with an RF-blanking for suppressing the noise during data acquisition. All experiments were performed using home built 5 mm solid state NMR probes. The probes were placed in a dynamic Oxford CF1200 helium flow cryostat. The sample temperature was controlled employing an Oxford ITC 503 temperature controller. During cooling and before and after data acquisition, the sample temperature was controlled directly *via* a CGR-1-1000 sensor placed in the direct vicinity of the sample.

† Crystallographic data have been deposited at the Cambridge Crystallographic Data Centre (CCDC). Enquiries for data can be directed to: Cambridge Crystallographic Data Centre, 12 Union Road, Cambridge, UK, CB2 1EZ or (e-mail) deposit@ccdc.cam.ac.uk or (fax) +44 (0)1223 336033. Any request to the CCDC for this material should quote the full literature citation and the reference number 1326/6. See http://www.rsc.org/suppdata/cp/1999/5113 for crystallographic files in .cif format.

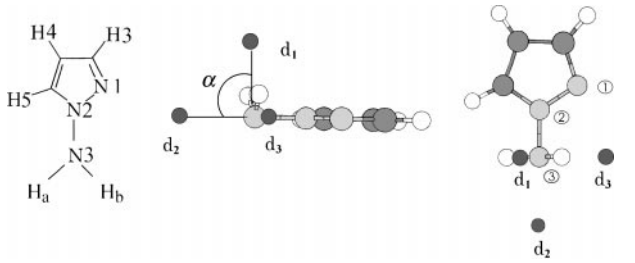

Scheme 2 Definition of the inversion (or pyramidalization) angle α and of the rotation angle ϕ. Inversion angle, $\alpha = 0°$ for planar NH_2 and $\alpha \neq 0°$ for a pyramidal NH_2. Rotation angle ϕ is defined by the dihedral angle N(1)–N(2)–N(3)–d_3. Position of the dummies: d_1, bissector of the H_a–N(3)–H_b angle; d_2–N(3)–N(2) is a straight line, and d_3 is perpendicular to the d_1–N(3)–d_2 plane through N(3).

This temperature was used to calibrate the readings of a second CGR-1-1000 sensor, which is part of the cryostat. During data acquisition, the first sensor was disconnected from the ITC 503 and grounded to protect the ITC from the RF and to avoid distortions of the signal. At each temperature, a delay of 30 min before the start of the NMR experiment was used after the nominal setting of the temperature to ensure the complete temperature equilibration and homogeneity of the sample. Typical 90° pulse widths were 3.0 μs for both ^1H and ^2H, corresponding to a B_1-field of 83 kHz in frequency units. All spectra were recorded using the solid echo technique, with an echo spacing of 30 μs. The repetition time of the experiments was between 10 and 60 s, depending on the T_1 relaxation time of the sample and the typical number of accumulations was 1600 scans per spectrum. ^1H NMR spectra have been recorded in the temperature range 180 to 270 K. ^2H NMR spectra of 1-aminopyrazole with a deuterated amino group have been recorded in the temperature range 143 to 257 K. Below 143 K T_1 became too long (>250 s) to record the signals. The spectra were measured starting at low temperatures to avoid supercooling of the compound.

^{15}N CPMAS NMR. The ^{15}N CPMAS (cross polarization magic angle spinning) NMR experiments were performed at two different fields, using a standard Bruker MSL 300 (7.1 T), 300.13 MHz for ^1H and 30.41 MHz for ^{15}N and a 5 mm Doty standard high speed CPMAS probe and a Bruker CXP 90 (2.1 T), 90.02 MHz for ^1H and 9.12 MHz for ^{15}N equipped with a 7 mm Doty standard probe. On both Bruker spectrometers a Bruker B-VT-1000 temperature unit was used to control the temperature of the bearing gas stream and a home-built heat exchanger to achieve low temperatures under MAS conditions. To avoid problems at low temperatures caused by air moisture, pure nitrogen from evaporating liquid nitrogen was used as bearing and driving gas. All chemical shifts are related to external solid $^{15}NH_4Cl$ and given with an error of ±0.3 ppm. Standard CPMAS spectra were measured using the usual CP pulse sequence.

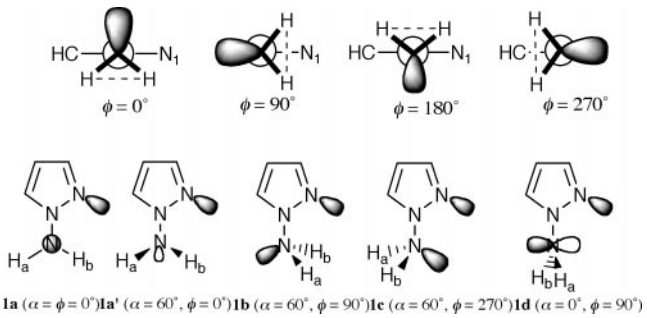

1a ($\alpha = \phi = 0°$)**1a'** ($\alpha = 60°$, $\phi = 0°$)**1b** ($\alpha = 60°$, $\phi = 90°$)**1c** ($\alpha = 60°$, $\phi = 270°$)**1d** ($\alpha = 0°$, $\phi = 90°$)

Scheme 3 Some illustrative examples of AMPZ conformational aspects for different values of the inversion (α) and rotation (ϕ) angles as defined in Scheme 2.

Low-temperature liquid state ^1H NMR spectroscopy. These experiments were performed on a 500 MHz Bruker NMR spectrometer AMX 500 using a deuterated freon mixture $CDClF_2$–CDF_3 (2 : 1) as solvent. The latter was synthesized from $CDCl_3$ as described previously.[15] The NMR samples were prepared using well-established vacuum techniques.

2.6 Computational details

In order to study the rotational and inversion dependence of the potential energy surface (PES) it is generally accepted that correlation effects have to be taken into account.[16] In our work we have explored the rotation–inversion PES for AMPZ **1** and aniline **2** in the framework of the density functional theory (DFT) using the B3LYP formalism[17] with a 6-31G* basis set for the geometry optimization. This formalism has been shown to give results in very good agreement with the *ab initio* results at the MP2 level,[18] and are less computationally intensive, which is important in our case given the size of the molecules and the number of points to be calculated. At all the points of the PES for each value of the inversion and rotation angle all the remaining geometrical parameters were fully optimized. Once the stationary points (minima and transition states) of this PES had been located, their geometries were fully reoptimized and their harmonic vibrational frequencies were evaluated at the same level of accuracy to estimate the zero point energy (ZPE). The results are available from the authors upon request. Single point calculations at the B3LYP/6-311+G(3df,2p)//B3LYP/6-31G* level were carried out for the minima and transition states in order to have reliable energetics, for the rotation and inversion barriers.

The definition of the inversion (α) and rotation (ϕ) angles varies from one author to another. α is the angle between the NH_2-plane and the aromatic ring, and ϕ, the angle between the HH vector and the aromatic ring, as illustrated in Scheme 2. In the case of sp^3 hybridization for the amino group, we represent in Scheme 3 the Newman's projections of AMPZ **1** for $\phi = 0$, 90, 180 and 270°. The most stable conformation, according to our previous calculations,[4,5] corresponds to **1b**, $\phi = 90°$. We also represent in Scheme 3 some limiting structures of AMPZ ($\alpha = 60°$ is an approximate value for sp^3 hybridization) that will be useful to discuss the potential energy surface, $E = f(\alpha, \phi)$. This surface contains several stationary points depending on the molecular structure.

3. Results

3.1 Theoretical calculations of the rotation-inversion surface of aniline and AMPZ

In Figs. 1 and 2 we give the calculated inversion–rotation potential energy surfaces (PES) for AMPZ and aniline, respectively. We note that in the case of AMPZ the global minimum occurs for a rotation angle $\phi = 90°$ and inversion angle $\alpha = 58°$ (structure **1b**) and the transition state (TS) for the rotational movement corresponds to $\phi = 0.0°$ and $\alpha = 60.5°$ (structure **1a'**). Hence, in this case the coupling between rotation and inversion is very weak. By contrast, in the case of aniline, the minimum corresponds to $\phi = 0.0$ and $\alpha = 42°$ and the barrier to rotation at $\phi = 90°$ and $\alpha = 53°$. In aniline, the rotation movement involves a stronger variation in the inversion angle. Leszczynski *et al.*[19] have calculated a barrier of 1.55 kcal mol^{-1} (for a TS at $\alpha = 42°$), which agrees better with the experimental value of 1.6 kcal mol^{-1}.[20]

In Figs. 3 and 4 we give the energy profile for the inversion in both systems. In the case of AMPZ an asymmetric double well is found, with the maximum for $\alpha = -0.6°$. The global minimum corresponds to the situation in which a plane through the nitrogen and hydrogen atoms of the amine group is perpendicular to the azole ring with the two hydrogens pointing towards the pyrazole nitrogen. In the aniline, due to the symmetry of the system, the profile is a symmetric double

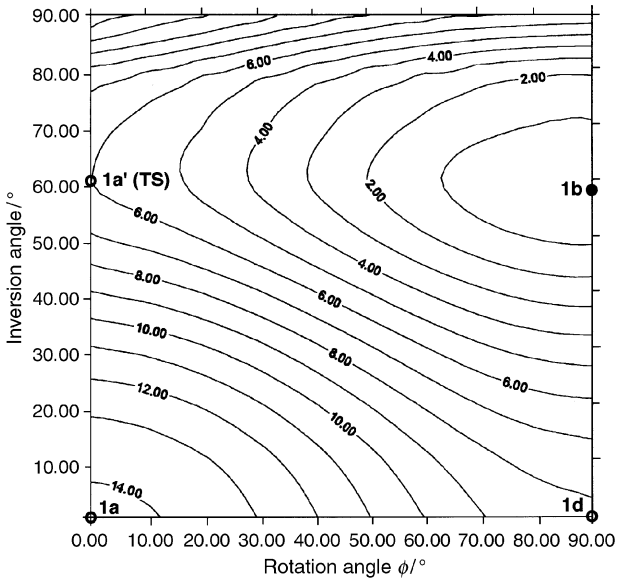

Fig. 1 Rotation–inversion PES in kcal mol^{-1} of AMPZ **1**. Absolute minimum (black point) at $\phi = 90°$ and $\alpha = 58°$.

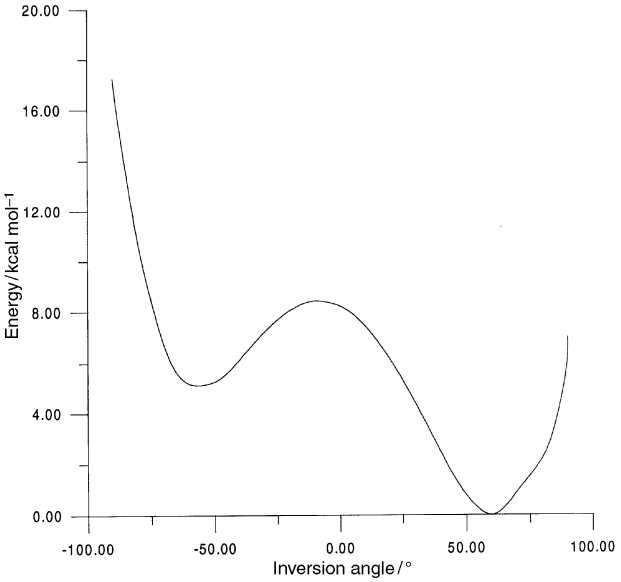

Fig. 3 Variation of the energy (in kcal mol^{-1}) as a function of the inversion angle α for AMPZ **1**. This asymmetric double well corresponds to the inversion keeping the rotation dihedral angle $\phi = 90°$ (the value of the global minimum of the rotation–inversion PES).

well with a very low barrier. In Table 1 we give the values of the rotation and inversion barriers obtained at the B3LYP/6-311+G(3df,2p) level. It can be observed that in the case of aniline the inversion barrier is only 0.11 kcal mol^{-1} if ZPE corrections are included, which means that at room temperature the inversion in this system would be barrier-free. For the case of AMPZ the situation is the opposite in the sense that the inversion barrier is higher than the rotational one.

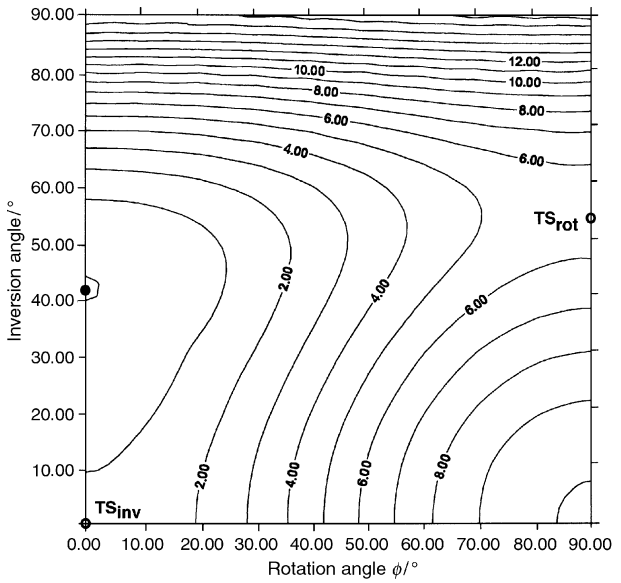

Fig. 2 Rotation–inversion PES in kcal mol^{-1} of aniline **2**. Absolute minimum (black point) at $\phi = 0°$ and $\alpha = 42°$.

3.2 Theoretical calculations of the hydrogen bond association of AMPZ

In principle, it would be necessary to study theoretically the influence of hydrogen bonding on the processes of inversion and rotation of the amino group. However, this problem

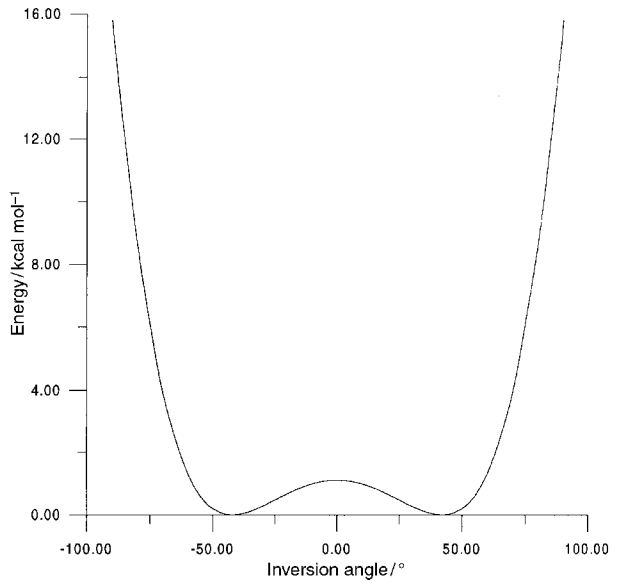

Fig. 4 Variation of the energy (in kcal mol^{-1}) as a function of the inversion angle α for aniline **2**. This symmetric double well corresponds to the inversion keeping the rotation dihedral angle $\phi = 0°$ (the value of the global minimum of the rotation–inversion PES).

Table 1 Total energies (E) in E_h at B3LYP/6-311+G(3df,2p)//B3LYP/6-31G*. Zero point vibrational energies (E_h) and rotational and inversion barriers (kcal mol^{-1}) for 1-aminopyrazole (AMPZ) and aniline[a]

	Aniline			AMPZ		
	Minimum	TS_{rot}	TS_{inv}	Minimum	TS_{rot}	TS_{inv}
E	−287.707 86	−287.698 43	−287.706 64	−281.626 81	−281.618 70	−281.616 49
ZPE	0.117 36	0.116 97	0.116 31	0.088 33	0.087 55	0.086 80
Inversion barrier[b]		0.11			5.51	
Rotational barrier[b]		5.67			4.79	

[a] 1 cal = 4.184 J. [b] Zero point energy corrections are included.

exceeds the scope of this study. Nevertheless, in order to get some indications of how the molecular structure of AMPZ is changed when the molecule associates we performed a B3LYP/6-31G* calculation of the dimer. The result is depicted in Scheme 4.

The dimer has a C_i symmetry (center of inversion ●) and corresponds to a pair of *anti* isomers **1b**. The amino group maintains its sp^3 hybridization (HNH angle = 106.5°) with $\alpha = 72.4°$ and $\phi = 90.0°$. The N(3)–H_b···N(1) hydrogen bond has the following characteristics: N(3)–H_b = 1.028 Å [N(3)–H_a = 1.021 Å], N(1)···H_b = 2.093 Å, N(3)–H_b···N(1) = 161.3°. The computed dimerization energy, including the ZPE correction, is 9.98 kcal mol^{-1}.

The main results from the theoretical calculations (Sections 3.1 and 3.2) concerning AMPZ are that the most stable conformation is **1b** ($\alpha = 58°$, $\phi = 90°$), that this conformation remains substantially unaltered by dimerization and that the barriers to either inversion or rotation are high, about 5 kcal mol^{-1} (Table 1 and Fig. 1).

3.3 X-ray structure, DSC properties and IR spectroscopy of AMPZ

The results of the X-ray structure analysis on solid 1-aminopyrazole are summarized in Fig. 5, which reveals that the molecules are held together by N–H···N hydrogen bonding interactions to form infinite columns running through the crystal, as is observed in solid pyrazole.[21–24] However, whereas the molecules of pyrazole form a simple chain made up of molecules linked by N–H···N hydrogen bonds in the form of an figure 8, aminopyrazole molecules pack with a three-dimensional network of hydrogen bonds passing along the center of the column.

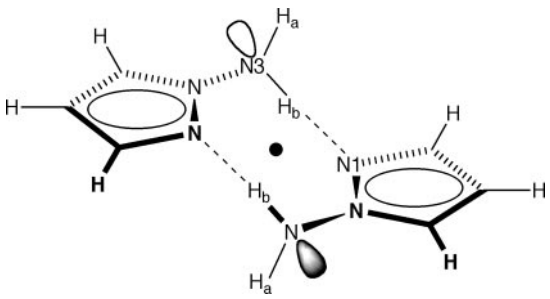

Scheme 4

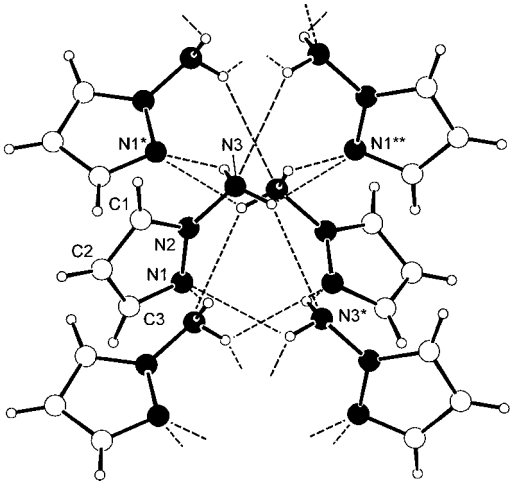

Fig. 5 Molecular structure of 1-aminopyrazole **1**, showing the N–H···N hydrogen bonding interactions (dashed lines indicate interatomic N···N distances less than 3.5 Å). Selected interatomic distances (Å) and angles (°): N(1)–C(3) 1.335(2), N(1)– N(2) 1.355(2), N(2)–N(3) 1.403(2), C(1)–N(2) 1.339(2), C(1)–C(2) 1.380(2), C(2)–C(3) 1.402(2), C(3)–N(1)–N(2) 103.8(1), N(1)–N(2)–C(1) 113.2(1), C(1)–N(2)–N(3) 124.8(1), N(1)–N(2)–N(3) 121.9(1), N(2)–C(1)–C(2) 106.7(1), C(1)–C(2)–C(3) 104.5(1), N(1)–C(3)–C(2) 111.9(1), N(3)···N(1*)[x, 0.5 − y, z − 0.5] 3.096(2), N(3)···N(3*)[− 0.5 − x, y, −0.5 + z] 3.451(2), N(3)···N(1**)[−0.5 − x, y, z − 0.5] 3.120(2).

The difference in the packing between aminopyrazole and pyrazole can be attributed to the fact that aminopyrazole has an additional N–H group available for hydrogen bonding. Each molecule of aminopyrazole carries two hydrogen bond donors (the H atoms of the NH_2 group) and two hydrogen bond acceptors (the lone pairs on the NH_2 group and on the ring =N– atom), and all of these functional groups participate in hydrogen bonding in the crystal. One of the hydrogen atoms of the NH_2 group at N(3) forms a hydrogen bond to the lone pair on N(1*) of a symmetry-related molecule (Fig. 5). The other proton interacts with the lone pair on N(3*) on a different molecule, with the hydrogen bond to the imine nitrogen lone pair being significantly shorter than that to the amine nitrogen atom [N···N 3.096(2) *vs.* 3.451(2) Å]. Since the molecules in the column are related by symmetry operations of the space group, the hydrogen bonding pattern is the same for each molecule.

A relatively short intermolecular distance between N(3) and N(1**) [3.120(2) Å] indicates that there may be an additional weak N–H···N interaction between these atoms, but it is probably not effective since the N–H···N angle of 117(2)° is significantly smaller than the other two N–H···N angles [N(3)–H···N(3*) 141(2) and N(3)–H···N(1*) 146(1)°]. The columns can be thought of as comprising a N–H···N hydrogen bonded core bound on two sides by hydrocarbon runners. As with pyrazole, each column is surrounded by six nearest neighbors, and the chains pack in a distorted hexagonally close-packed arrrangement.

Apart from the hydrogen atoms on the amine group, the aminopyrazole molecule is planar (rms deviation from the mean plane 0.018 Å) and bond distances and angles are comparable with those in similar molecules.[22] The nitrogen atom of the NH_2 group in 1-aminopyrazole, 1-amino-3-phenylpyrazole and 1-amino-3-phenyl-5-methyl-pyrazole[25] all have sp^3 character. Based on the positions of the hydrogen atoms, the nitrogen atom lone pairs in all three compounds are oriented approximately *antiperiplanar* to the N–N bond in the ring (**1b**, $\phi = 90°$, Scheme 3), in accord with the theoretical calculations on the parent molecule (see previous discussion and ref. 4). In AMPZ the torsion angles for the two hydrogen atoms of the amine group N(1)–N(2)–N(3)–H are 46(2) and − 67(2)°. The asymmetry can be attributed to the constraints of molecular packing and hydrogen bonding to the other molecules in the column. The arrangement causes the molecules to be chiral. The columns are made up of alternately left- and right-handed molecules.

Aniline, in contrast to aminopyrazole, has only one nitrogen lone pair available to accept a hydrogen bond. As a result, in solid aniline[26] only one of the hydrogen atoms of the NH_2 group is involved in hydrogen bonding to a neighboring molecule. The molecules are linked by single N–H···N hydrogen bonds to form infinite chains extending through the crystal. The low symmetry of the crystal means that one finds two independent N–H···N interactions in the solid, but the corresponding N···N distances [3.180(6) and 3.373(5) Å] are comparable with those found in the structure of 1-aminopyrazole (Fig. 5). Although N–H···N interactions dominate the packing in many aminopyrazoles, it is worth noting that the hydrogen bonding pattern is influenced by substituents in the ring.[25]

The different HB network between aniline and AMPZ is also apparent in their IR spectra (liquids between two disks of NaCl). While aniline shows bands at 3433 (νNH_{as}) and 3364 cm^{-1} (νNH_s) which follow the Bellamy–Williams–Hambly relationship ($\nu NH_s = 0.7033 \nu NH_{as} + 948.2$)[27,28] this is no longer the case for AMPZ. This compound shows two bands at 3314 and 3197 cm^{-1}. For the AMPZ dimer, calculations

(Section 3.2) yield the following values (scaled by a 0.98 factor): 3426 (two degenerate modes, ν_{as}), 3302 (ν_s-out-of-phase) and 3290 cm^{-1} (ν_s-in phase).

The DSC thermogram (Fig. 6) is relevant for the NMR neat experiments. It shows that AMPZ solidifies at −48.5 °C, has a very small solid–solid transition at −44.3 °C and melts at −1.5 °C; afterwards it resolidifies at −42.2 °C, has the phase transition at −43.5 °C and melts at −0.76 °C. The solid–solid transition is difficult to observe and in other experiments (scan speed 5 °C min^{-1}) it was not found: the sample crystallized cleanly at −53.6 °C and melted again at −0.76 °C.

3.4 ^{1}H NMR solution studies of AMPZ labelled with ^{15}N on the amino group

We have recorded the ^{1}H NMR of [^{15}N]AMPZ in a 1 : 2 mixture of CDF_3 and CDF_2Cl between 105 and 150 K at 500 MHz. The results are depicted in Fig. 7.

Besides the peaks of residual solvent CHF_3 and CHF_2Cl marked by asterisks we observe three peaks for the hydrogen nuclei H(5), H(3) and H(4) bound to carbon at 7.43, 7.3 and 6.1 ppm. Their chemical shifts depend only slightly on temperature, whereas the chemical shift of the amino protons strongly depends on the latter. At about the highest temperatures where experiments were performed a well resolved doublet is observed around 6.7 ppm for both protons of the amino group, characterized by a coupling constant of $^1J(^1H–^{15}N) = 71$ Hz.[4] When temperature is lowered the doublet is shifted downfield which strongly indicates that the amino group of AMPZ forms hydrogen bonds preferentially at low temperatures. At very low temperatures the amino doublet broadens in such a way that it becomes almost lost in the base line; in addition, the C–H signals also broaden. Unfortunately, it was not possible even at around 100 K to reach the slow hydrogen bond exchange regime where the two amino protons, H_a and H_b, should exhibit different chemical shifts. Therefore, within the NMR time scale, hydrogen bond exchange is fast in the liquid state.

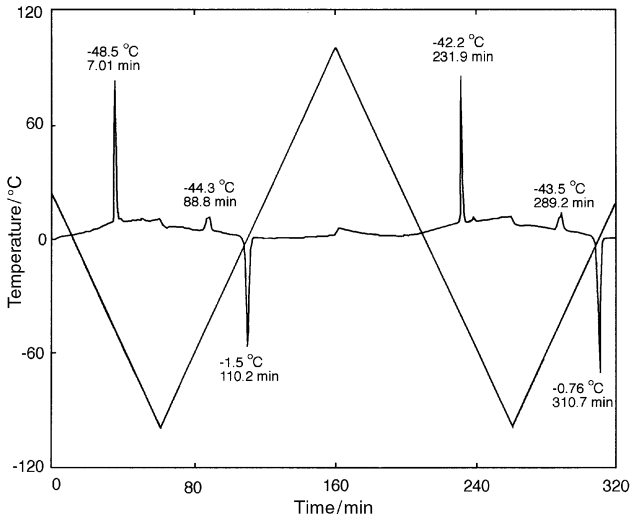

Fig. 6 DSC thermogram of AMPZ **1**.

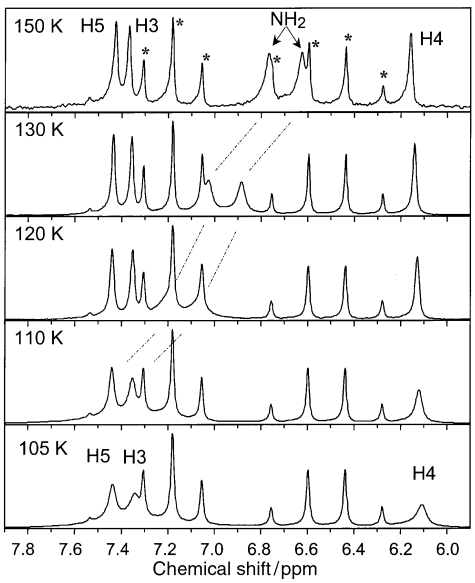

Fig. 7 Evolution of the ^{1}H NMR spectrum of [^{15}N]AMPZ with the temperature (values in ppm, solvent CDF_3–CDF_2Cl 1 : 2). * Signals due to the undeuterated solvents.

3.5 Solid state ^{2}H NMR and ^{15}N CPMAS NMR of AMPZ

Two different types of solid state NMR studies have been performed on the AMPZ, namely ^{1}H and ^{2}H measurements on non-rotating samples and ^{15}N measurements on a rotating sample using the CPMAS technique.

Fig. 8 displays the ^{2}H spectra, recorded in the temperature range 143 to 257 K. At low temperatures (143 to 213 K) the ^{2}H NMR line shape is practically independent of the temperature and corresponds to a typical ^{2}H NMR spectrum with $q_{cc} = 202 \pm 4$ kHz and $\eta = 0.16 \pm 0.02$. At 219 K the spectrum becomes very noisy, indicating a very short T_2 time at this temperature. Above this temperature, the signal-to-noise ratio becomes better again and two lines are visible, a narrow one in the center indicating a very mobile or liquid-like component and a broad component, similar to the low temperature line. Upon further increase of the temperature, the relative intensity of the narrow component increases until at 257 K the broad component has disappeared and only the narrow line has survived.

Fig. 9 shows the ^{1}H solid state NMR spectra of AMPZ measured between 180 and 270 K. Even at low temperatures the signals are relatively narrow for ^{1}H NMR spectra of non-rotating solids (*ca.* 40 kHz at 180 K). In the spectra, there is a change of the line shape in the range from 210 to 250 K and then, on heating, a rather narrow liquid-like component appears, together with the broad component.

The static ^{1}H and ^{2}H measurements yield information about the dynamics of the AMPZ in the solid state. The short ^{2}H T_2 value at 219 K suggests that a motion of the AMPZ or the $–ND_2$ group is on the time scale of the echo delay and thus interferes with the NMR experiment. While this motion is frozen below 200 it is active in the spectra at higher temperatures. The coexistence of the narrow and the broad component in the temperature range between 220 and 248 K suggests that two different types of AMPZ molecules are present in the sample, namely immobile ones (broad

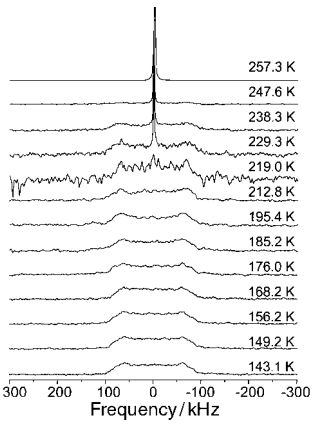

Fig. 8 ^{2}H NMR powder spectra of [ND_2]AMPZ.

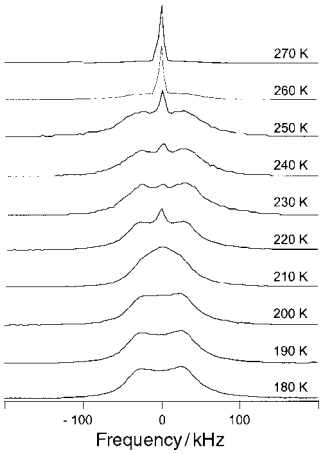

Fig. 9 ^{1}H NMR powder spectra of AMPZ.

component) and highly mobile ones (narrow component). This result is corroborated by the ^{1}H NMR spectra, where the change of the line shape in the temperature range between 210 and 270 K is observed. In principle there are two different explanations for this behavior, namely (a) a phase separation has occurred in the sample, *i.e.* while part of the sample is still solid another part is already in a liquid-like state; or (b) the AMPZ exhibits a glassy behavior, *i.e.* a broad distribution of rotational correlation times.

Fig. 10 shows the ^{15}N CPMAS NMR spectra of AMPZ, labelled at the nitrogen atom of the amino group, measured at 193, 173 and 153 K at a field of 2.1 T (9.12 MHz). At room temperature, AMPZ is a liquid and gives a narrow ^{15}N line at 43.6 ppm (7.1 T, 30.41 MHz).

4. Discussion

The main computational result for AMPZ is that this molecule possesses an amino group conformation close to $\alpha = 60°$, $\phi = 90°$ (**1b**), that is, sp^3 hybridized and with an HH axis perpendicular to the aromatic ring. By contrast, in the case of aniline, this axis is parallel ($\phi = 0°$) to the molecular plane and amino group hybridization somewhere between sp^2 and sp^3 ($\alpha = 42°$). Another difference is that in AMPZ the rotation–inversion barriers are uncoupled and high, near 5 kcal mol^{-1}, while in aniline they are coupled and weak, about 1 kcal mol^{-1}. In the form **1b**, to interconvert H_a and H_b involves a combined rotation and inversion *via* **1a** as intermediate. This makes AMPZ a very different compound from aniline, and from 2-aminopyridine ($\alpha = 15.9°$, $\phi = 1.5°$) where the amino group is sp^2 hybridized and planar.[6] Association by hydrogen bonds does not modify significantly the values of the α and ϕ angles in AMPZ, therefore, the dimer can be described in good approximation as consisting of two **1b** monomers linked by two N(3)–H···N(1) hydrogen bonds (HB) as shown in Scheme 4. The dynamics of H_a/H_b interconversion in the dimer was not studied, but it should proceed either by HB dissociation or by a HB switch. It is important to notice that the plane of symmetry present in **1b** is a consequence of H_a and H_b being isochronous, while in the dimer they become anisochronous because only one of them is involved in an HB.

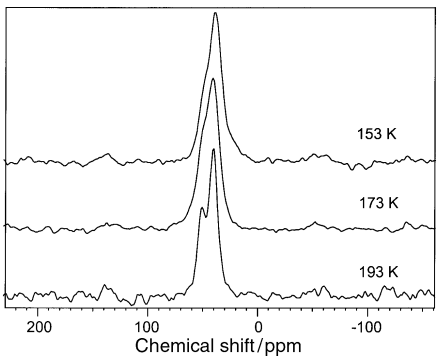

Fig. 10 ^{15}N CPMAS NMR at 2.1 T of [^{15}N]AMPZ.

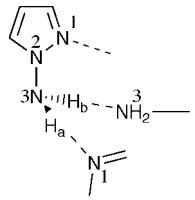

Scheme 5

Liquid state ^{1}H NMR shows equivalent H_a and H_b, consistent with $\phi = 90°$, in the whole temperature range down to 110 K. When the temperature decreases, the signal of the amino NH_2 protons shifts to low field, indicating dominating monomers at high temperatures and H-bonded associates at low ones. The observation of a ^{1}H–^{15}N scalar coupling proves that in these conditions the proton exchange is slow. The value of the coupling constant is 71 Hz (Section 3.4), independent of temperature and hydrogen bonding, *i.e.*, much smaller than the corresponding coupling constant in aniline, 78.9 Hz (absolute value).[29] This reduction is understandable in terms of the sp^3 hybridization of AMPZ which is almost not affected by H bonding. The type of HB associates could not be determined. The H_a/H_b isochrony is maintained down to 110 K, *i.e.* H-bond switches fast in the associates which is consistent with an H-bond dimer energy of 10 kcal mol^{-1} (Section 3.2), that is, about 5 kcal mol^{-1} per HB.

In the solid state, DSC shows the presence of two crystal phases, the molecular structure of the low temperature one was determined by X-ray crystallography. AMPZ has two HB donor sites, H_a and H_b, and two acceptor ones, N(1) and N(3). The calculated dimer uses only two, H_a and N(1). In the crystal, following the principle of maximizing the number of HBs,[30] all four are used, as represented in Scheme 5. Clearly, H_a and H_b are inequivalent which is consistent with the presence in IR of two NH stretchings.

^{2}H and ^{1}H solid state NMR confirm the existence of two solid phases. (1) A low temperature phase where the N–H vectors are fixed in space. The quadrupolar coupling constant of ^{2}H is normal. These constants are almost the same for H_a and H_b, therefore, ^{2}H NMR spectroscopy cannot detect the anisochrony of H_a and H_b. (2) A high temperature phase for which ^{2}H and ^{1}H NMR spectra show that the whole molecule is subject to fast isotropic reorientation. The ^{15}N CPMAS results of AMPZ monolabelled with ^{15}N on the amino group show that the signal of N(3) is split into an asymmetric doublet due to residual dipolar interaction with ^{14}N(2).[31]

5. Conclusions

This paper has demonstrated the very unusual structure of AMPZ **1** with $\phi = 90°$ and $\alpha = 60°$ leading to equivalent amino protons, equivalence maintained when AMPZ forms hydrogen bonds in liquid and solid in contrast with aniline **2** and 2-aminopyridine **3**.

Acknowledgements

This work was supported by the European Community Human Capital & Mobility Network "Localization and Transfer of Hydrogen" (No. CHRX CT 940582) and the DGICYT of Spain (Project number PB 96-0001-C03). H.H.L. thanks the Fonds der Chemischen Industrie, Frankfurt, for

financial support. We also thank Dr Consuelo Escolástico (UNED) for recording the DSC thermogram and Dr Ilja G. Shenderovich (Berlin) for performing the low-temperature NMR solution experiments.

References

1 J. Elguero, *Pyrazoles and their Benzo Derivatives*, in *Comprehensive Heterocyclic Chemistry*, ed. A. R. Katritzky and C. W. Rees, Pergamon Press; Oxford, 1984, vol. 5, p. 167; J. Elguero, *Pyrazoles*, in *Comprehensive Heterocyclic Chemistry II*, ed. A. R. Katritzky, C. W. Rees and E. F. Scriven, Pergamon, Oxford, 1996, vol. 3, p. 1.
2 T. Kauffmann, *Angew. Chem., Int. Ed. Engl.*, 1971, **10**, 743.
3 V. V. Kuzmenko and A. F. Pozharskii, *Adv. Heterocycl. Chem.*, 1992, **53**, 85.
4 C. Foces-Foces, F. H. Cano, R. M. Claramunt, D. Sanz, J. Catalán, F. Fabero, A. Fruchier and J. Elguero, *J. Chem. Soc., Perkin Trans. 2*, 1990, 237.
5 O. Mó, M. Yáñez, A. L. Llamas-Saiz, C. Foces-Foces and J. Elguero, *Tetrahedron*, 1995, **51**, 7045.
6 M. Chao, E. Schempp and R. D. Rosenstein, *Acta Crystallogr., Sect. B*, 1975, **31**, 2922.
7 G. Barbieri, R. Benassi, R. Grandi, U. M. Pagnoni and F. Taddei. *J. Chem. Soc., Perkin Trans. 2*, 1979, 330.
8 K. Inuzuka and A. Fujimoto, *Bull. Chem. Soc. Jpn.*, 1992, **65**, 1002; K. Inuzuka, *Nippon Kagaku Kaishi*, 1997, 100; K. Inuzuka, *Nippon Kagaku Kaishi*, 1997, 393.
9 M. W. Rathke and A. A. Millard, *Org. Synth., Coll. Vol. VI*, 1988, 943.
10 H. Neunhoeffer, M. Clausen, H. D. Vötter, H. Ohl, C. Krüger and K. Angermund, *Liebigs Ann. Chem.*, 1985, 1732.
11 F. Aguilar-Parrilla, R. M. Claramunt, C. López, D. Sanz, H.-H. Limbach and J. Elguero, *J. Phys. Chem.*, 1994, **98**, 8752.
12 G. M. Sheldrick, *Acta Crystallogr., Sect. A*, 1990, **46**, 467.
13 SHELXL-97, Sheldrick, G. M., University of Göttingen, 1997.
14 G. Buntkowsky, I. Sack, H.-H. Limbach, B. Kling and J. Fuhrhop, *J. Phys. Chem. B.*, 1997, **101**, 11265.
15 S. N. Smirnov, N. S. Golubev, G. S. Denisov, H. Benedict, P.Schah-Mohammedi and H.-H. Limbach, *J. Am. Chem. Soc.*, 1996, **118**, 4094 and references therein.
16 W. J. Hehre, L. Radom, P. v. R. Schleyer and J. A. Pople, in *Ab Initio Molecular Orbital Theory*, John Wiley, New York, 1986 and references therein.
17 A. D. Becke, *J. Chem. Phys.*, 1993, **98**, 5648; C. Lee, W. Yang and R. G. Parr, *Phys. Rev.*, 1988, **B37**, 785.
18 L. Gonzalez, O. Mó and M. Yáñez, *J. Comput. Chem.*, 1997, **18**, 1124; L. Gonzalez, O. Mó, M. Yáñez and J. Elguero, *J. Mol. Struct.: THEOCHEM.*, 1996, **371**, 1.
19 O. Bludsky, J. Sponer, J. Leszczynski, V. Spirko and P. Hobza, *J. Chem. Phys.*, 1996, **105**, 11042.
20 J. C. Brand, D. R. Williams and T. J. Cook, *J. Mol. Spectrosc.*, 1966, **20**, 359.
21 H. W. W. Ehrlich, *Acta Crystallogr.*, 1960, **4**, 946.
22 J. Berthou, J. Elguero and C. Rérat, *Acta Crystallogr., Sect. B*, 1970, **26**, 1880.
23 F. K. Larsen, M. S. Lehmann, I. Sotøfte and S. E. Rasmussen, *Acta Chem. Scand.*, 1970, **24**, 3248.
24 T. La Cour and S. E. Rasmussen, *Acta Chem. Scand.*, 1973, **27**, 1845.
25 K. Yamaguchi, A. Ohsawa, T. Kaihoh, M. Okada, C. Kawabata and H. Igeta, *Acta Crystallogr., Sect. C*, 1989, **45**, 1902.
26 M. Fukuyo, K. Hirotsu and T. Higuchi, *Acta Crystallogr., Sect. B*, 1982, **38**, 640.
27 L. K. Dyall, *Spectrochim. Acta, Part A*, 1988, **44**, 283.
28 L. K. Dyall, G. L'abbé and W. Dehaen, *Spectrochim. Acta, Part A*, 1997, **53**, 377.
29 R. E. Wasylishen and T. Schaefer, *Can. J. Chem.*, 1973, **51**, 3087.
30 G. R. Desiraju, in *Crystal Engineering. The Design of Organic Solids*, Elsevier, Amsterdam, 1989, p. 125; J. Bernstein, M. C. Etter and L. Leiserowitz, in *Structure Correlation*, ed. H.-B. Bürgi and J. D. Dunitz, VCH, Weinheim, 1994, vol. 2, p. 431.
31 S. H. Alarcón, J. A. Jiménez, R. M. Claramunt, H.-H. Limbach and J. Elguero, *Magn. Reson. Chem.*, submitted.

Paper 9/06187H